International Journal of Innovative Engineering Applications

Journal homepage: https://dergipark.org.tr/ijiea

PRODUCTION AND CHARACTERIZATION OF COMPOSITE POWDER FROM MEDIUM ENTROPY ALLOYS PRODUCED USING W, Mo, Nb – Fe, Ni, Co POWDERS

Muhammet Gökhan Albayrak*[1]

[1]*Firat University, Faculty of Engineering, Department of Metallurgical and Materials Engineering, Elazig/Turkey*

Abstract

Original scientific paper

Todays, Middle Entropy Alloys (MEA) are a relatively new production method and have extraordinary advantages over classical methods. The biggest advantage is defined as the production of complex compounds that cannot be combined with known methods. MEAs prepared with transition metals such as Fe, Ni, Co have an important place due to their superior properties such as anti-oxidation, corrosion and wear behavior. Metals with refractory properties such as W, Mo, Nb are interesting due to their high hardness as well as high temperature applications. In this study, which aims to characterize two different MEA powders produced, MEA powders were produced using refractory metals such as W, Mo and Nb and transition metal powders such as Fe, Ni and Co. The difference of this publication is that all powders are not brought together at once during production, but W, Mo, Nb and Fe, Ni, Co powders are produced separately and combined later. Mechanical Alloying (MA) was preferred as the production method due to its advantages such as reducing grain size and ensuring chemical homogenization. XRD, SEM and EDS (mapping) analyses were performed for the characterization of the obtained medium entropy alloy composite. Thanks to the MA technique, the powder sizes were reduced and both MEA powders were successfully distributed homogeneously within each other.

Keywords: *Characterization, complex compounds, FeNiCo, middle entropy alloy, WMoNb.*

W, Mo, Nb – Fe, Ni, Co TOZLARI KULLANILARAK ÜRETİLEN ORTA ENTROPİ ALAŞIMLARINDAN KOMPOZİT TOZ ÜRETİMİ VE KARAKTERİZASYONU

Özet

Orijinal bilimsel makale

Orta Entropi Alaşımları (MEA) günümüzde oldukça yeni bir üretim metodu olup klasik üretimlere göre sıradışı avantajlara sahiptir. Bilinen yöntemlerle bir araya gelemeyen kompleks bileşiklerin üretilmesi en büyük avantajı olarak tanımlanmaktadır. Fe,Ni, Co gibi geçiş metalleriyle hazırlanan MEA 'lar anti-oksidasyon, korozyon ve aşınma davranışı gibi üstün özellikleri sebebiyle önemli bir yere sahiptir. Refrakter özellikleri bulunan metaller örneğin W, Mo, Nb, yüksek sıcaklık uygulamalarının yanısıra sahip oldukları yüksek sertlikten dolayı ilgi çekicidir. Üretilen iki farklı MEA tozlarının karakterizasyonunu amaçlayan bu çalışmada W, Mo ve Nb gibi refrakter metaller ile Fe, Ni ve Co gibi geçiş metal tozları kullanılarak MEA tozları üretilmiştir. Üretim esnasında bütün tozların tek seferde bir araya getirilmeyip sırasıyla W, Mo, Nb ve Fe, Ni, Co tozlarının ayrı ayrı üretilip sonradan birleştirilmesi bu yayının farkını oluşturmaktadır. Tane boyutunun düşürülebilmesi ve kimyasal olarak homojenizasyonun sağlanabilmesi gibi üstünlüklerinden dolayı üretim yöntemi olarak Mekanik Alaşımlama (MA) tercih edilmiştir. Elde edilen orta entropi alaşım kompozitinin karakterizasyonu için XRD, SEM ve EDS (haritalama) analizleri yapılmıştır. MA tekniği sayesinde, toz boyutları azaltılmış ve her iki MEA tozu birbiri içerisinde homojen olarak başarıyla dağıtılabilmiştir.

Anahtar Kelimeler: *FeNiCo, karakterizasyon, kompleks bileşikler, orta entropi alaşımı, WMoNb.*

1 Introduction

Traditionally, an alloy is composed of a dominant primary element and modicum amounts of secondary ones added [1]. These additions should not be random, but should be determined and processed according to a certain knowledge or experience, resulting in improved material properties for different industries. Because it is the secondary ones that give the alloy desired and various differences [2].

A new approach to alloying was mentioned in a study published in 2004 [3]. This new approach focuses on the intermediate regions of the known and traditionally accepted multicomponent phase diagrams, instead of

*Corresponding author.

E-mail address: mgalbayrak@firat.edu.tr (M. G. Albayrak)

Received 27 February 2025; Received in revised form 16 April 2025; Accepted 21 May 2025

 Doi: https://doi.org/10.46460/ijiea.1648175

focusing on their entirety. The fact that the focused regions consist of unexplored compositional areas represents a significant conceptual change due to the risks associated with phase stability. These differences are the most unique aspect of the new approach [4]. Since study published in 2004 is different from conventional methods, it has the feature of inspiring scientists in their studies today. Therefore, in this study, the term "High Entropy Alloys" (HEA) was used for the first time. HEAs are defined on two principles. The first of these is the principle of having no atom less than 5% and more than 35% (Eq. 1) on the basis of atomic percentage (X_i), and having a total of 5 major metallic elements (n_{major}).

$$n_{major} \geq 5, \qquad 5 \leq X_i \leq 35 \qquad \text{(Eq. 1)[3]}$$

HEAs' have an arrangement of elements in a particular form and combination entropy, the second one, greater than 1.5 R ($R = 8{,}314 J/mol.K$) in the random solution state. For an alloy with "*n*" elements in a random solution state, the ordered combination entropy per mole (ΔS_{conf}) is calculated by the addition equation (Eq. 2).

$$\Delta S_{conf} = -R \sum_{i=1}^{n} X_i ln X_i \qquad \text{(Eq. 2)[3]}$$

The R value of a HEA containing 5 equiatomic metallic elements is calculated as 1.61. For this reason, the R value of 1.5 is accepted as the lower limit for HEAs containing 5 equiatomic metallic elements [5]. Continuing with this definition, the range of 1-1.5 R is called Medium Entropy Alloy (MEA), and 1 R and below is called Low Entropy Alloy (LEA) [6]. The entropy distribution according to the number of co-atomic elements calculated according to Eq. 3 is given in Table 1. "*n*" indicates the quantity of participants (metallic elements) and "ΔS_{Conf}" indicates the entropy value.

Table 1. ΔS_{Conf} distributions according to the number of co-atomic elements.

n	*1*	*2*	*3*	*4*	*5*	*6*	*7*	*8*	*9*
ΔS_{Con}	0	0.69R	1.1R	1.39R	1.61R	1.79R	1.95R	2.08R	2.2R

All alloys which are high, medium and low entropy should be selected on an appropriate scale to modify the microstructure and to be used in different combinations (non-isoatomic). In non-homoatomic low entropy alloys the microstructure is very variable. All (Single or Multi)-Phase microstructures including equiatomic and non-equiatomic phases are formed by high-entropy alloys [7].

The elements in the periodic table have various effects on entropy alloys. In general, the group 1 alkaline elements (excluding the hydrogen elements) have high levels of reactivity [8]. Group 2 elements (Alkaline Earth Metals), are preferred in lightweight HEAs because they can provide weight savings due to their low density [9]. The elements found in groups 3-12 (except Ac) are called transition metals. In addition to its strengths such as thermal and electrical conductivity, D block (transition metals) also has oxidation resistance. Thus, it is quite successful in preventing corrosion of metal parts in the system in which it is used. Post-transition metals that have high affinity to neighboring metals [10]. Metalloids exhibit both metallic and non-metallic behavior and moreover are generally used in HEAs to increase the strength and ductility of the FCC crystal structure [11]. Metalloids find use in structural improvement and biomedical sector applications [12]. The addition of nonmetals with low atomic radius such as C, N, O, P, S, and Se increases the hardness and decreases the toughness of the Fe alloy system. Due to the presence of 4f electrons with greater bonding strength in nature, Lanthanide group elements known Rare Earth Elements (REE) are used in applications where increased hardness and strength are required.

Based on the results of the studies, one of the most suitable ways to reduce particle size, refine grain size and achieve these without compromising chemical homogeneity is undoubtedly the mechanical alloying (MA) technique [13], [14]. MA, also known as high-energy ball alloying, is formed during mechanical alloying by mechanochemical reactions involving solid-solid and solid-liquid interactions. Based on the two different types of reactions in grinding conditions, the self-propagating combustion reaction promotes high enthalpy during grinding. Another incremental reaction occurs gradually. The important parameters affecting MA are ball-powder ratio, powder volume, container volume, grinding speed, grinding time, ball material, ball diameter, number of balls used and process control agents. In Figure 1, the MA jar and the breaking and re-boiling of the powder particles during MA are also schematically illustrated on the figure. If we need to explain the parameters affecting MA, the ball-powder ratio describes the weight ratio of the ball and powder in the container. Alloying speed and duration form the basis of the process. The material of the ball and the material of the container must not create a pollutant in the dust in case of wear. It is important to choose the same or similar material as the powder as possible. The ball diameter and number affect the weight of the ball used. Process control substances refer to a liquid to be given along with a gas or powder that will fill the space in the container. Increased product life or durability is a result of mechanical alloying or powder crushing aimed at improving mechanical performance. Injecting additives increases their effectiveness in the mechanical alloying process. These additives are called Process Control Agents (PCAs). PCAs are surfactants, sometimes known as surface additives. PCAs can be liquid or solid [10].

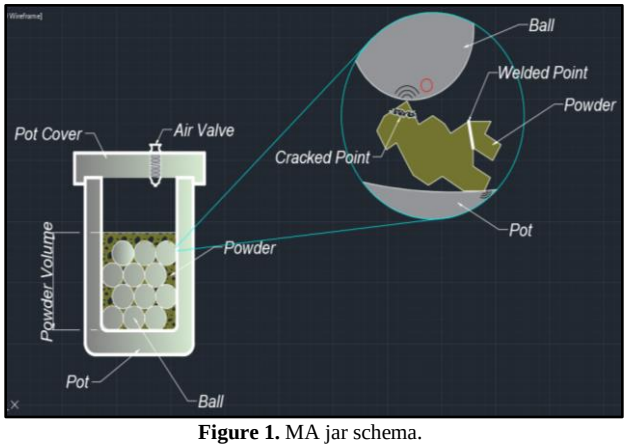

Figure 1. MA jar schema.

Due to the metal term originating from the HEA definition, FeNiCo is frequently used by scientists in MEA production. This combination, which attracts attention due to its mechanical and magnetic properties, is especially investigated in solving energy-related sector problems [15]. Although it has been shown that magnetic properties can be improved by producing FeNiCo-based alloys with different combinations (e.g. FeNiCoMnCu [16], FeNiCoMnAl [17], FeNiCoAlSi [18]), the mechanical properties are not at the desired levels [19]. On the other hand, it has been reported in the literature that composite HEA/MEA produced with particle reinforcements such as oxide or carbide give better results than alloys combined with chemical composition [20], [21]. Until 2010, while alloys based on transition metals such as Fe, Ni and Co were frequently studied in the literature, it is known that HEAs based on refractory composition elements were not discovered [22]. A new window has been opened for scientists with the use of elements such as W, Mo, Nb with refractory characteristics. It is also known that BCC HEAs have higher hardness than FCCs. Additionally, it has been discovered over the years that refractory HEAs have high mechanical properties in addition to their thermal properties [22], [23]. Indeed, providing entropy stability at high temperatures by being added to materials with ductility [24]–[26] and creating wear resistance due to having higher hardness than transition metals [27], [28] are some of the best examples of this new window. It is also becoming worth examining in the exploration of refractory metals. However, it was determined that there was no MEA prepared with W, Nb and Mo, which are among the refractory metals frequently researched in the literature.

In this study, two different MEAs which were FeNiCo and WMoNb, were produced. Then FeNiCo and WMoNb powders were weighed 95% and 5% by weight, respectively. These alloys were subjected to homogenization in a mechanical mill for another 5 hours to ensure both the necessary homogeneity and become a composite. Mechanical alloying (MA) was preferred as the production method in order to benefit from the advantages it provides in both MEA production. Characterization tests of both MEAs were performed and the study was completed by examining the final MEA mixture composite in terms of homogenization. The aim of this study is to produce a composite powder with two different MEAs and to characterize both MEAs and composite powders.

2 Material and Method

The elemental powders to be used in the study were commercially supplied by Nanografi company, provided that they were of high purity. Equal atomic W (Nanografi Company, 99.95% purity, 10µm), Mo (Nanografi Company, 99.99% purity, 10µm), Nb (Nanografi Company, 99.95% purity, 10µm), Fe (Nanografi Company, 99.99% purity, 5µm), Ni (Nanografi Company, 99.99% purity, 10µm) and Co (Nanografi Company, 99.9% purity, 10µm) powders were weighed on a precision balance and then grouped as WMoNb and FeNiCo. RETSCH PM200 device was used in the mechanical alloying process. The pot and balls used were selected as stainless steel, the ball-powder ratio was 10:1, and the rotation speed was 300 rpm, in the Ar atmosphere. The WMoNb group was commanded to work for 120 hours, with a 30-minute break every 30 minutes and the next work to be in the opposite direction, while the FeNiCo group differed from the previous group only in that the process lasted for 30 hours. Due to the presence of high hardness elements such as W, the MA period was determined as a long period of 120 hours in order to reduce the grain size and achieve proper homogenity. For relatively softer powders such as Fe, Ni and Co, MA treatment for a longer time such as 120 h was avoided because it could cause undesirable effects such as agglomeration in the powders. The production phase was completed by subjecting the obtained powder groups to a 5-hour final process under the same environment and conditions as above in order to ensure structural homogeneity. Whole MA process was carried out inert atmosphere (Ar, 99,999% purity) The production process of the study is schematized in Figure 2. Rigaku Miniflex 600 was used for X-Ray Diffraction (XRD) analysis, Hitachi SU3500 for Scanning Electron Microscopy (SEM) analysis and Oxford AZtech for Electron Dispersive Spectroscopy (EDS) analysis for powder characterization.

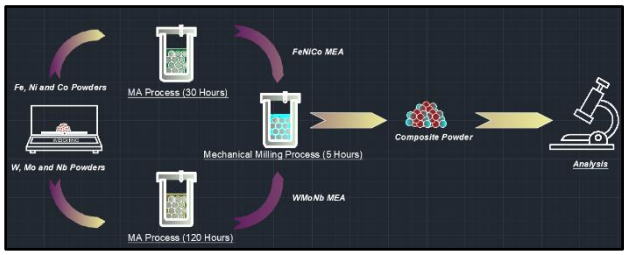

Figure 2. Production process of the study.

3 Results and Discussion

3.1 XRD Analyses of the Samples

During the preparation of the produced powder composite, two different groups were created, then these two different groups were brought together and powder characterizations were performed both as a group and as a single composite. The XRD graph of WMoNb produced as the first group MEA is given in Figure 3. The WMoNb powder mixture prepared as equiatomic was subjected to 120 hours of MA treatment and is named as "*WMoNb MA 120h*" in the figure. The reference codes used in XRD analyses were W *(Ref Code: 00-004-0806)*, Mo *(Ref Code: 00-042-1120)* and Nb *(Ref Code: 00-016-0001)*, respectively. For W, peaks of 40.265° (110), 58.276° (200), 73.198° (211) and 87.024° (220), for Mo, also peaks, 40,516° (110), 58,609° (200), 73,684° (211) and 87,598° (310) were observed. Nb peaks were also detected at 38.610° (110), 55.697° (200), 69.701° (211) and 82.524° (220).

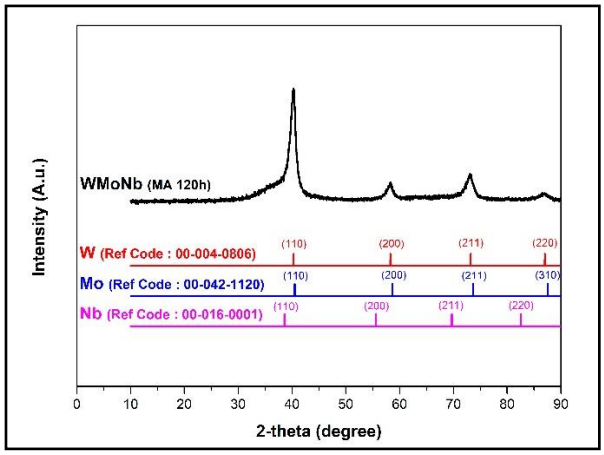

Figure 3: XRD analysis of WMoNb MEA.

The XRD analysis of FeNiCo MEA, which forms the second group of the composite, is given in Figure 4. Just like in the previous group, the results named "*FeNiCo MA 0h*" and "*FeNiCo MA 30h*" are shown before and after the MA process of the FeNiCo powder prepared as identical atoms, respectively. Before the process, the characteristic peaks of Fe (Ref Code: 00-001-1262), Ni (Ref Code: 00-045-1027) and Co (Ref Code: 00-001-1277) are clearly seen. It is observed that there is a decrease in peak intensities after 30 hours of MA treatment. The decrease in peak intensities and angular misalignments required by the MA process are examples of situations encountered in the literature [29]. Although some of the angular differences are based on the device used for measurement, it is generally a phenomenon that is read together with the success of the MA process. Similar situations have been encountered in our previous studies [30]. As seen in Figure 4, before mechanical alloying, FeNiCo powder exhibits pronounced and strong peaks. When looking at *Reference Codes* (Ref Code) to which the XRD data belong, it is seen that the cubic structures are not disrupted. The MA process causes marked alterations in the crystal structure of WMoNb powders. A distinct degredation in the intensity of XRD pattern is observed at all compositions for both the first and second groups. The characteristic peaks of Fe, Ni and Co at 44.6° (110), 44.52° (011) and 47.31° (101), respectively, are still observable, but their intensity has broadened and decreased significantly.

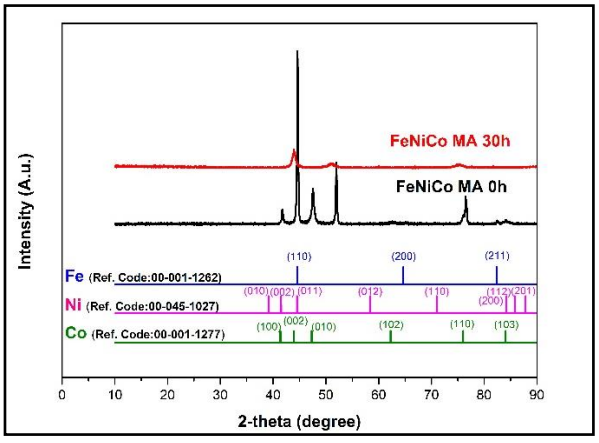

Figure 4. XRD analysis of FeNiCo MEA.

In Figure 5, XRD analyses of WMoNb and FeNiCo powders, in addition to 5% reinforced WMoNb and 95% FeNiCo composite powders are given together. In order to obtain a homogeneous distribution for a total of 5 hours by combining the two groups, the MA process was repeated without altering the environment and circumstances of the first two groups. The composite is named as "WMoNb + FeNiCo". While WMoNb has a very low concentration of 5%, it is inevitable that FeNiCo powder dominates in the XRD analysis of the composite powder. However, the peak of WMoNb around 40 degrees is also seen in the powder composite.

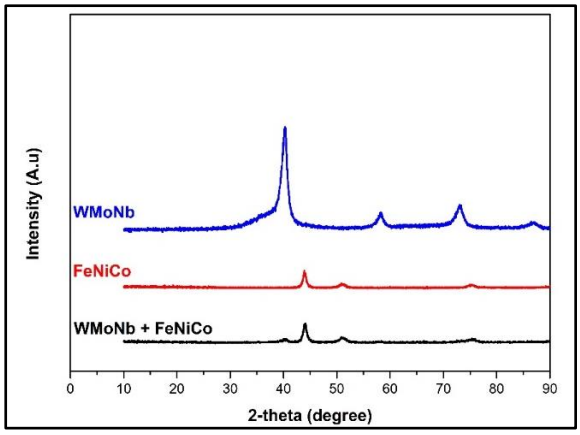

Figure 5. XRD analysis of WMoNb, FeNiCo and WMoNb + FeNiCo MEAs.

This expansion can be explained in two ways. The first one is the reduction in grain size. The second one is the increase in lattice tension. Both explanations are characteristic of the high-energy milling process and indicate that the powders have undergone this process. Angular deviations and expansions are observed at the peak positions. This is a phenomenon reported in the literature. It is considered as repeated fracture and cold welding caused by the powder being stayed in between ball-ball or ball-wall. This repeated randomly oriented fracture and welding process is consistent with previous reports of mechanical alloying, which leads to defect formation and lattice distortion. The substantial decline in peak intensity following MA process (see Figure 3) shows the success of the process related to MA on the crystalline structure of the composite powders. The decline in crystallinity index (see Table 2) is evidence of the mutation from an ordered crystalline to a more disordered possibly named somewhere-amorphous, state due to the high strain induced by mechanical alloying [31], [32]. It is reported in the literature [33] that MA can reduce grain sizes from micron to nano level and cause the emergence of high density dislocations and other defects due to structural deterioration. [30].

Table 2. Average grain size, crystallinity index and average dislocation density belog to all samples.

Samples	***Before MA Process***			***After MA Process***		
	Grain Size	*C. Index*	*D. Density*	*Grain Size*	*C. Index*	*D. Density*
FeNiCo	32.41258	47.84 %	0.000952	8.053712	23.21 %	0.015417
WMoNb	-	-	-	0.138699	57.96 %	51.98204
	Before Mixing for Homogenization			***After Mixing for Homogenization***		
Composite	7.65796	46.61 %	0.059599	0.13867	29.09 %	52.00379

While creating Table 2 containing Average Grain Size and Average Dislocation Density, "*Origin Pro 8.5*" software and "*Scherrer Equation* (Eq.3) [34]" were used. For composite, "*Before Mixing for Homogenization*" sections were calculated by averaging grain size.

$$D = \frac{k.\lambda}{\beta_{hkl}.cos\theta_{hkl}} \quad \text{(Eq.3)}$$

"*D*" symbolizes Grain Size. "*k*" Shape Factor and "λ" Wavelength are constants that are 0,9, and 0,154, respectively. "β" represents the Full Weight at Half Maximum (FWHM) value calculated from the peaks in the XRD image and with "$cos\theta$", it is the radian value of the 2-theta degree of the peak intensity.

The Crystallinity Index (Eq.4) [35] and Dislocation Density (Eq.5) [30] values were also calculated via XRD images. Formulation of these are below (Eq.4 and 5.);

$$\text{Crystallinity Index} = \frac{\text{Area of all the crystalline peaks}}{\text{Area of all crystalline and amorphous peaks}} \quad \text{(Eq.4)}$$

$$\delta = \frac{1}{D^2} \quad \text{(Eq.5)}$$

Average grain size and crystallinity index data have critically decreased after MA process. However, dislocation density has increased as expected. As seen in Table 2, time of MA process is primarily responsible for this situation.

3.2 SEM Analysis of the Composite Powders

SEM images of FeNiCo MEA a) before alloying and b) after alloying are given in Figure 6. It can be clearly seen from the images that the grain size is reduced. This conclusion can be reached as a result of mechanical grinding.

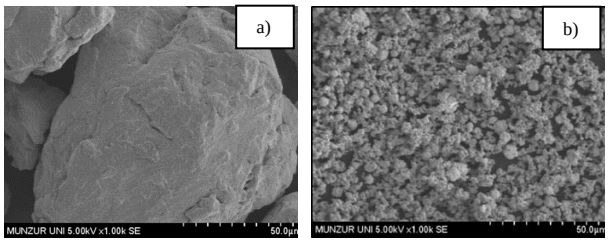

Figure 6. SEM images of FeNiCo MEA a) before alloying and b) after alloying.

Figure 7 shows SEM images of WMoNb MEA a) before alloying and b) after alloying. While it is observed that the powder size decreases with the mechanical alloying process, it is observed that the size distribution within the structure is not homogeneous. This situation is interpreted as the powders starting to agglomerate as a result of the high-energy alloying environment for a long time such as 120 hours. Although non-homogeneous powder particle distribution was mentioned above, this agglomeration is a physical volume increase other than chemical bonding.

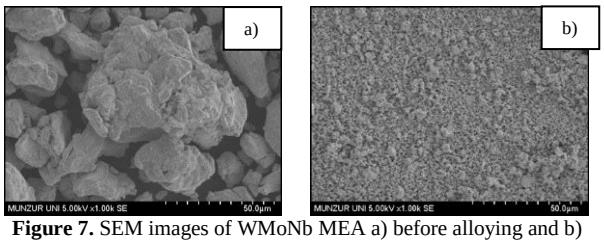

Figure 7. SEM images of WMoNb MEA a) before alloying and b) after alloying.

SEM image of WMoNb + FeNiCo composite is given in Figure 8. The powder, stayed between the ball-ball or ball-wall collusion is broken locally by the energy of the balls (caused by centrifugal force). Then, in another ball-ball or ball-wall collision, cold welding of the powders stayed in randomly between and overlapping each other occurs. By reducing the powder size, an advantage is gained for the sintering process carried out in advanced stages of powder metallurgy [36]–[38]. The possibility of approaching the desired optimum values in mechanical properties with low powder size increases. Lower particle size means lower porosity and therefore improved packing density. In this way, an increase in hardness and strength as well as an improvement in wear resistance can be achieved.

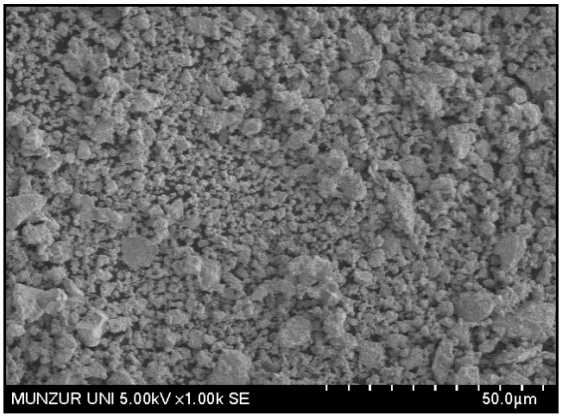

Figure 8. SEM image of WMoNb + FeNiCo composite.

Similar to Figure 7, it is seen in Figure 8 that the particle sizes are not homogeneous among themselves (FeNiCo and WMoNb). This situation can be explained by two reasons. The first of these is the agglomeration that occurs as a result of high-energy alloying, as in the WMoNb powder. In the study conducted by Ji et al. [39], it was stated that agglomerations started at MA times of 60 hours and above. The second is that although the mixing process is carried out for 5 hours under the same conditions for the purpose of homogenization, the grain sizes of the powders may differ from each other due to the different MA times. In addition, the agglomeration of the powders due to the difference in powder grain sizes can be added to the list as a third factor, albeit weak.

3.3 EDS Analysis of the Composite Powders

EDS analysis of FeNiCo MEA is given in Figure 9. It is also seen in the EDS analysis image that the dust size decreases according to the applied MA process. In addition, it is observed that Fe, Ni and Co mixed as elemental powder are mixed homogeneously

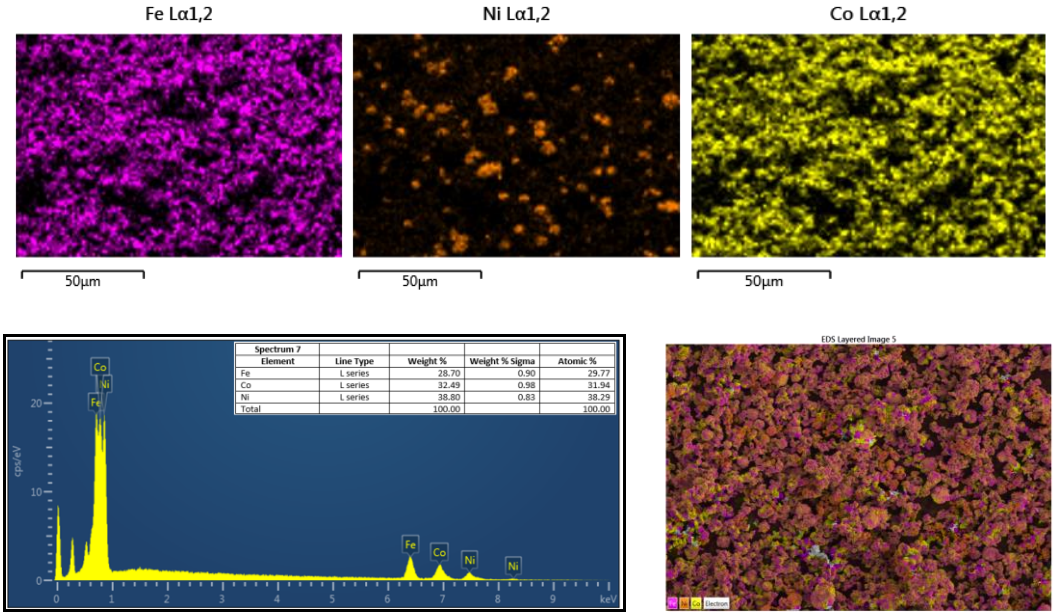

Figure 9. EDS analysis of FeNiCo MEA.

In Figure 10, the EDS analysis of the powder composite of WMoNb and FeNiCo MEA is given. As a result of the 5-hour mixing process in order to ensure a homogeneous distribution in both MEAs, it is seen that the structure is homogeneously distributed in the EDS images.

These findings are in line with the expected results and demonstrate the successful fabrication of the targeted MEA. SEM and elemental mapping analyses elucidate the microstructure of the fabricated MEAs. The dominance of particle sizes below 5 µm and the homogeneous distribution of constituent metals with atomic ratios ranging from 4.5% to 5.5% underline the meticulous control over the fabrication process. With this study, it was seen that homogeneous distributions can be obtained without melting, as in the studies carried out with full melting in the literature [40]–[42]. It is very clear that different advantages can be obtained with this MEA production (with MA process), which enables the metals with low and/or high melting temperatures to be brought together without melting.

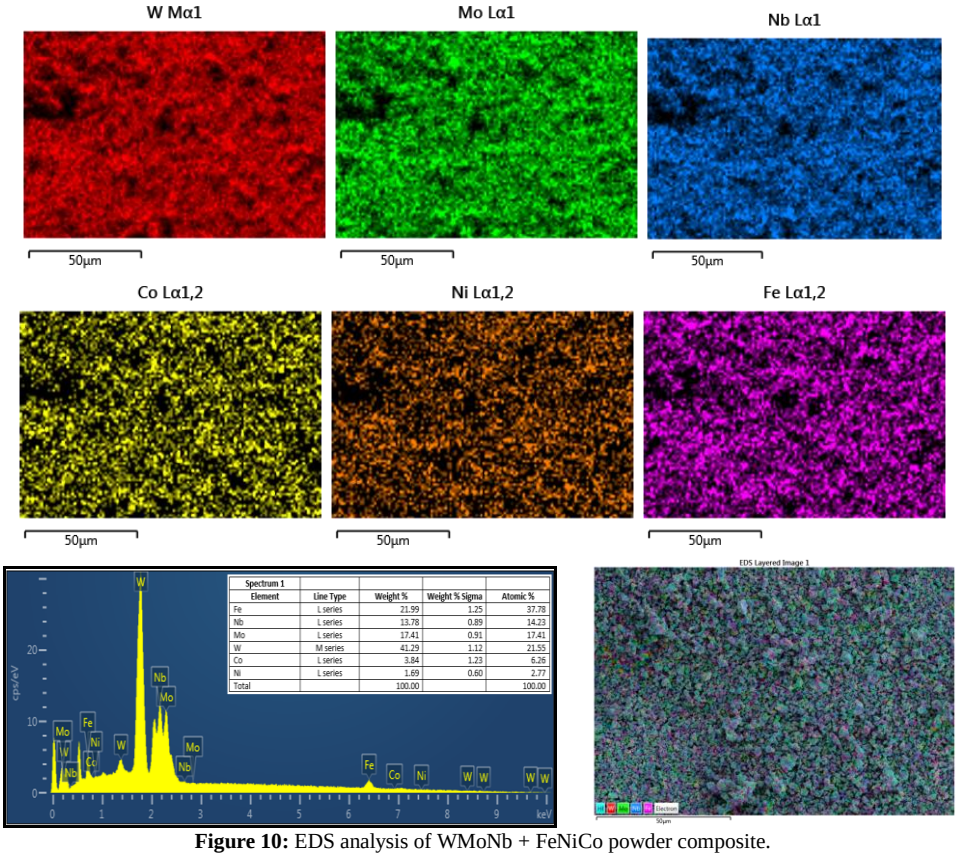

Figure 10: EDS analysis of WMoNb + FeNiCo powder composite.

4 Conclusion

The mechanical production of the powders of both groups (Fe, Ni, Co and W, Mo, Nb) weighed as equal atoms was completed in the MA device. MA process was applied to FeNiCo and WMoNb powders for 30 and 120 hours, respectively, and two different MEA powder productions were successfully completed. Then, a 5-hour Mechanical Milling process was carried out to make these two groups a composite and to homogenize the structure. XRD, SEM and EDS analyses were performed for the powder characterization of the composite. Thus;

In the XRD analysis, it was determined that the dislocation density of both groups increased. It was seen that the peak heights decreased and the openness increased. Thus, it was revealed that the structure started to change from a regular state to an amorphous state with the MA performed. It is also seen that the FeNiCo powder, which is more in weight, is still dominant in the composite. With SEM analysis, it was clearly observed that the MA process reduced the grain size after 120 and 30 hours of MA processing. With EDS analysis, the powders were visualized as elementally homogeneous in both MEA and composite powder production.

As a result, the production of two different MEA powder groups as a composite was successfully achieved. It was revealed that MEA reinforcement can be made instead of particles to particle-reinforced MEAs, which are included in the literature, and that this can be produced successfully.

Declaration

Ethics committee approval is not required.

References

[1] Gorsse, S., Couzinié, J. P., & Miracle, D. B. (2018). From high-entropy alloys to complex concentrated alloys. *Comptes Rendus Physique, 19*(8), 721–736.

[2] Youssef, K. M., Zaddach, A. J., Niu, C., Irving, D. L., & Koch, C. C. (2014). A novel low-density, high-hardness, high-entropy alloy with close-packed single-phase nanocrystalline structures. *Materials Research Letters, 3*(2), 95–99.

[3] Yeh, J. W., Chen, S. K., Lin, S. J., Gan, J. Y., Chin, T. S., Shun, T. T., ... & Chang, S. Y. (2004). Nanostructured high-entropy alloys with multiple principal elements: Novel alloy design concepts and outcomes. *Advanced Engineering Materials, 6*(5), 299–303.

[4] Cabrera, M., Oropesa, Y., Sanhueza, J. P., Tuninetti, V., & Oñate, A. (2024). Multicomponent alloys design and mechanical response: From high entropy alloys to complex concentrated alloys. *Materials Science and Engineering R Reports, 161*.

[5] Yeh, J. W. (2015). Physical metallurgy of high-entropy alloys. *JOM, 67*(10), 2254–2261.

[6] Yeh, J. W. (2013). Alloy design strategies and future trends in high-entropy alloys. *JOM, 65*(12), 1759–1771.

[7] Gupta, M. (n.d.). Multiple component alloys: The way forward in alloy design. *Materials Science Research India, 16*, 1.

[8] Dye, J. L. (2015). The alkali metals: 200 years of surprises. *Philosophical Transactions of the Royal Society A, 373*(2037).

[9] Emsley, J. (2011). *Nature's building blocks: An A–Z guide to the elements* (New edition). London: Oxford University Press.

[10] B. V., & A. X. M. (2024). Development of high entropy alloys (HEAs): Current trends. *Heliyon, 10*(7), e26464.

[11] Wei, D., et al. (2022). Metalloid substitution elevates simultaneously the strength and ductility of face-centered-cubic high-entropy alloys. *Acta Materialia, 225*, 117571.

[12] Sekhon, B. S. (2013). Metalloid compounds as drugs. *Research in Pharmaceutical Sciences, 8*(3), 145–158.

[13] Yang, D., et al. (2020). A novel FeCrNiAlTi-based high entropy alloy strengthened by refined grains. *Journal of Alloys and Compounds, 823*, 153729.

[14] Udhayabanu, V., Singh, N., & Murty, B. S. (2010). Mechanical activation of aluminothermic reduction of NiO by high energy ball milling. *Journal of Alloys and Compounds, 497*(1–2), 142–146.

[15] Gutfleisch, O., Willard, M. A., Brück, E., Chen, C. H., Sankar, S. G., & Liu, J. P. (2011). Magnetic materials and devices for the 21st century: Stronger, lighter, and more energy efficient. *Advanced Materials, 23*(7), 821–842.

[16] Fu, Z., et al. (2019). Exceptional combination of soft magnetic and mechanical properties in a heterostructured high-entropy composite. *Applied Materials Today, 15*, 590–598.

[17] Zuo, T., et al. (2017). Tailoring magnetic behavior of CoFeMnNiX (X = Al, Cr, Ga, and Sn) high entropy alloys by metal doping. *Acta Materialia, 130*, 10–18.

[18] Zhang, Y., Zuo, T., Cheng, Y., & Liaw, P. K. (2013). High-entropy alloys with high saturation magnetization, electrical resistivity, and malleability. *Scientific Reports, 3*, 1–7.

[19] Chu, C., et al. (2023). Unveiling heterogeneous microstructure and good combinations of high yield strength and low coercivity of in-situ formed NbC/FeNiCo medium-entropy composites. *Powder Technology, 419*, 118365.

[20] Song, B., et al. (2020). In situ oxidation studies of high-entropy alloy nanoparticles. *ACS Nano, 14*(11), 15131–15143.

[21] Wu, H., Huang, S., Qiu, H., Zhu, H., & Xie, Z. (2019). Effect of Si and C additions on the reaction mechanism and mechanical properties of FeCrNiCu high entropy alloy. *Scientific Reports, 9*(1), 1–10.

[22] Senkov, O. N., Wilks, G. B., Miracle, D. B., Chuang, C. P., & Liaw, P. K. (2010). Refractory high-entropy alloys. *Intermetallics, 18*(9), 1758–1765.

[23] Zhang, B., Huang, Y., Huang, Z., & Wang, J. (2025). Porous WMoTaNb refractory high entropy alloy fabricated by elemental powder metallurgy. *Materials Today Communications, 45*, 112362.

[24] Senkov, O. N., Wilks, G. B., Scott, J. M., & Miracle, D. B. (2011). Mechanical properties of Nb25Mo25Ta25W25 and V20Nb20Mo20Ta20W20 refractory high entropy alloys. *Intermetallics, 19*(5), 698–706.

[25] Yao, H. W., Qiao, J. W., Hawk, J. A., Zhou, H. F., Chen, M. W., & Gao, M. C. (2017). Mechanical properties of refractory high-entropy alloys: Experiments and modeling. *Journal of Alloys and Compounds, 696*, 1139–1150.

[26] Dangwal, S., & Edalati, K. (2025). Developing a single-phase and nanograined refractory high-entropy alloy ZrHfNbTaW with ultrahigh hardness by phase transformation via high-pressure torsion. *Journal of Alloys and Compounds, 1010*, 178274.

[27] Stepanov, N. D., Shaysultanov, D. G., Salishchev, G. A., & Tikhonovsky, M. A. (2015). Structure and mechanical properties of a light-weight AlNbTiV high entropy alloy. *Materials Letters, 142*, 153–155.

[28] Senkov, O. N., & Woodward, C. F. (2011). Microstructure and properties of a refractory NbCrMo0.5Ta0.5TiZr alloy. *Materials Science and Engineering A, 529*(1), 311–320.

[29] Zhang, K. B., Fu, Z. Y., Zhang, J. Y., Wang, W. M., Lee, S. W., & Niihara, K. (2010). Characterization of nanocrystalline CoCrFeNiTiAl high-entropy solid solution processed by mechanical alloying. *Journal of Alloys and Compounds*, *495*(1), 33–38.

[30] Albayrak, M. G., & Evin, E. (2023). A different approach: Effect of mechanical alloying on pack boronizing. *Journal of Materials Engineering and Performance*, *33*, 9039–9046.

[31] Chen, C. L., & Zeng, Y. (2016). Synthesis and characteristics of W–Ti alloy dispersed with $Y_2Ti_2O_7$ oxides. *International Journal of Refractory Metals and Hard Materials*, *56*, 104–109.

[32] Wang, C., Ji, W., & Fu, Z. (2014). Mechanical alloying and spark plasma sintering of CoCrFeNiMnAl high-entropy alloy. *Advanced Powder Technology*, *25*(4), 1334–1338.

[33] Chen, C. L., & Suprianto. (2019). Effects of nano-dispersoids on synthesis and characterization of low Cr-containing CoNiFeMnCr high entropy alloy by mechanical alloying. *Intermetallics*, *113*, 106570.

[34] Suryanarayana, C., & Norton, M. G. (1998). *X-ray diffraction: A practical approach*. New York: Plenum Publishing Corporation.

[35] Tarani, E., Arvanitidis, I., Christofilos, D., Bikiaris, D. N., Chrissafis, K., & Vourlias, G. (2023). Calculation of the degree of crystallinity of HDPE/GNPs nanocomposites by using various experimental techniques: A comparative study. *Journal of Materials Science*, *58*(4), 1621–1639.

[36] Fang, Z. Z., Wang, H., & Kumar, V. (2017). Coarsening, densification, and grain growth during sintering of nano-sized powders—A perspective. *International Journal of Refractory Metals and Hard Materials*, *62*, 110–117.

[37] Yan, M. F., Cannon, R. M., Bowen, H. K., & Chowdhry, U. (1983). Effect of grain size distribution on sintered density. *Materials Science and Engineering*, *60*(3), 275–281.

[38] Sendi, R. (2022). Grain size and sintering temperatures effects on the mechanical properties of ZnO nanoparticle-based varistor ceramics. *Journal of Umm Al-Qura University for Applied Sciences*, *8*(1–2), 50–56.

[39] Ji, W., et al. (2015). Alloying behavior and novel properties of CoCrFeNiMn high-entropy alloy fabricated by mechanical alloying and spark plasma sintering. *Intermetallics*, *56*, 24–27.

[40] Wang, W., Lyu, T., Choi, H. S., Cheng, C., & Zou, Y. (2025). Wear mechanism transitions in FeCoNi and CrCoNi medium-entropy alloys from room temperature to 1000 °C. *Journal of Materials Science and Technology*, *231*, 151–163.

[41] Cao, F., et al. (2024). Carbon-microalloying enhances strength-ductility synergy of (FeCoNi)90Al10 medium-entropy alloy via tailoring precipitation. *Materials Science and Engineering A*, *916*, 147329.

[42] Wang, X., Suo, H., Zhang, Z., Huangfu, S., & Wang, Q. (2024). Exploring the effect of Cr and Mn on the intrinsic strength of the tensile properties of FeCoNi, FeCoNiMn, FeCoNiCr, and FeCoNiCrMn multi-principal element alloys using in-situ EBSD. *Materials Science and Engineering A*, *918*, 147442.

.